

Blind Modulation Format Recognition for Software-defined Optical Networks Using Image Processing Techniques

Tianwai Bo*, Jin Tang, and Calvin Chun-Kit Chan

Department of Information Engineering, The Chinese University of Hong Kong, Shatin, N.T., Hong Kong SAR

Author e-mail address: tianwai@ie.cuhk.edu.hk

Abstract: A novel modulation format recognition algorithm based on connected component analysis in binary image processing is proposed and verified by both simulation and experiment. It shows high accuracy and much reduced complexity than conventional clustering-based method.

OCIS codes: (060.0060) Fiber optics and optical communications, (060.4080) Modulation

1. Introduction

Recently, management of optical networks is progressing more flexible and software-defined. Fully programmable bandwidth variable transponders are adaptive to the data rate and the modulation format, based on the transmission length and channel state information so as to increase the spectral efficiency and assure the quality of service. In particular, it is highly desirable to have the receivers being able to automatically recognize the signal's modulation format, hence proper digital signal processing (DSP) algorithm can be applied to achieve the optimum performance for the received optical signal. Another application that requires modulation format recognition (MFR) is the coherent burst mode transmission system, in which the coherent receiver is required to respond to the fast channel switching. Several MFR schemes have been proposed, recently [1-3]. Among them the Stokes space based algorithms [3] are promising as they were inherently tolerant to carrier phase noise, frequency offset as well as polarization mixing. However, these methods are based on the computation-extensive iterative K-means or expectation maximization methods, which hinder their practical implementation.

In this paper, we propose a new non-iterative MFR method using very simple and fundamental image processing technique. By projecting the received samples in the 3-dimensional (3D) Stokes space to a 2D binary image with very small size, simple connected component analysis (CCA) [4] is employed to recognize the modulation format. All the operations on the complex numbers are now replaced by logic operations, as there are only 0 and 1 in the binary image, hence the computation complexity is drastically reduced. Numerical simulations and experiments show that by utilizing a few number of received symbols, simple and fast modulation format recognition functionality for coherent receiver can be achieved.

2. Principles

At the coherent receiver, it is common to perform analog-to-digital conversion, chromatic dispersion compensation and timing recovery, before handling the modulation format. After these pre-processing, in our proposed blind modulation recognition scheme, the dual polarization signal is first converted to the Stokes space, by [4]

$$[s_1, s_2, s_3] = [|X|^2 - |Y|^2, 2\text{Re}\{X \cdot Y^*\}, 2\text{Im}\{X \cdot Y^*\}] \quad (1)$$

where X and Y represent the two orthogonal polarizations, while $\text{Re}\{\cdot\}$ and $\text{Im}\{\cdot\}$ stand for the real and the imaginary parts of a complex number, respectively. As the absolute phase information has been removed in the transformation, the laser frequency offset and carrier phase noise has no effect in the Stokes vector space. Phase-shift-keying (PSK) signals have constant amplitude, which ensures a zero s_1 value. As seen in Fig. 1(a) and (b), the PSK signals distribute on the s_2 - s_3 plane ($s_1=0$). If we project the 3-dimensional (3-D) Stokes vector space to a 2-D plane, parallel to the s_2 - s_3 plane, we obtain the constellation diagram, as shown in Fig. 1(e) and (f) for QPSK and 8PSK, respectively. For the quadrature amplitude modulation (QAM) signal, the amplitude is not constant, and its distribution on the 3-D Stokes space is complicated. Fig 1(c) illustrates the distribution of a polarization multiplexed (PM) 16QAM signal, which has 60 clusters of points. As seen in Fig. 1(g), simply projecting these points to s_2 - s_3 plane cannot differentiate each constellation point easily, even at relatively large signal-to-noise ratio (SNR), due to the small Euclidean distance. In principle, 16QAM has three different amplitudes, thus the theoretical values of s_1 after transformation and normalization are $\{-4/9, -2/9, 0, 2/9, 4/9\}$. This distribution can be clearly seen, if we rotate Fig. 1(c) with a certain angle of view, as in Fig. 1(d). If we only project the outermost two symmetric plane (p_2 and p_2') to the s_2 - s_3 plane, a simple four-point constellation can be obtained. It should be noted that the random polarization walk needs to be tracked and rotated to its initial state in Stokes space so as to have the optimum

sensitivity. The calculation of polarization rotation matrix (RM) in Stokes space is much easier than the polarization demultiplexing process in the Jones space, and modulation format independent [5]. This polarization RM can be used as an initial state for the subsequent polarization demultiplexing equalizers, in which the complexity reduction can be more than an order of magnitude than the conventional constant modulus algorithm, as demonstrated in [5]. The MFR is still performed before the polarization demultiplexing.

Before generating the graph, the noise-corrupted signal should be filtered first, based on the density of distribution on the projection plane. Here, we employ the Voronoi polygon method other than using a square or circular mask to estimate the dot density, in order to simplify the calculation of density. For each specific point (named “seed”) in a point set, we can find such a polygon, that all the points inside this polygon is more closer to this seed other than any other seeds. This polygon is called Voronoi cell. The vertices of the cell can be found efficiently through the Fortune’s algorithm [6] with a complexity of $O(n \cdot \log(n))$. The inverse value of the cell area can be used to estimate the density of each seed. Then, only the seed with its area smaller than a certain threshold remains and the rest is filtered out. Fig. 2(a) is a Voronoi diagram of an 8PSK constellation with a SNR of 18 dB, and Fig. 2(b) illustrates the survival points after density-based filtering with points whose normalized density smaller than 0.6 being removed. Then we convert the survived points in the constellation diagram to a binary graph, with a defined resolution N . It first normalizes the values in s_2 and s_3 to $[0, 1]$ and fits them in an $N \times N$ grid. If there is any point falling into the grid, the grid is assigned with value “1”, otherwise it is “0”. The grid procedure is analogous to “quantization” in digital communication system, after which an $N \times N$ binary graph is obtained, as shown in Fig. 2(c). To smooth out the graph, an averaging filter is used. Fig. 2(d) shows the binary graph after the averaging filter. Finally, the connected component analysis is employed to count the number of constellation points. It traverses each pixel with value “1” (white color in Fig. 2(c) and (d)) in the graph and checks whether it is connected to any of the surrounding 8 pixels. It quickly labels all the connected subsets in a binary graph with only one time search [6]. Therefore the complexity is $O(n)$. After labelling all the subsets, the number of subsets is obtained, obviously. The modulation format recognition is achieved based on the number of subsets. For the received symbols, we use two binary image, generated from data sets (s_1, s_2, s_3) with $|s_j| < 0.11$ and $|s_j| > 0.33$, respectively. QPSK and 8PSK do not have samples in the latter image, thus are recognized by the number of subsets in the former image, while 16QAM should have four subsets in the latter image. The detailed algorithm design is shown in Fig. 3(a).

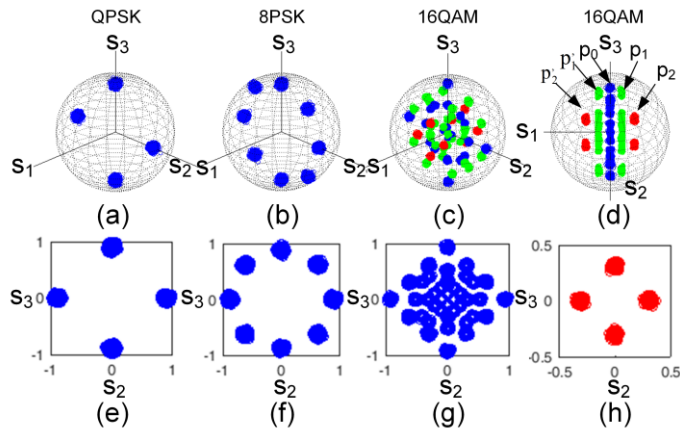


Fig. 1. Signal representations in Stokes space for (a) QPSK, (b) 8PSK, (c) 16QAM. (d) 16QAM as well, but in a different angle of view. (e)-(h) are the projections on the plane of s_2 - s_3 plane.

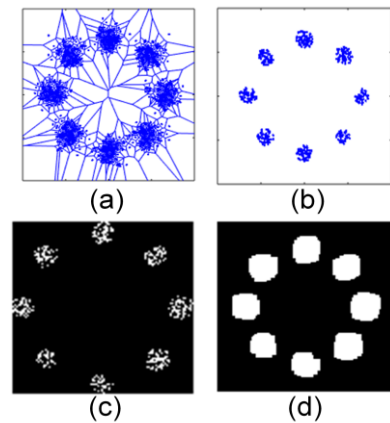


Fig. 2 (a) Voronoi diagram of the S_2 - S_3 projection of a PM-8PSK signal with SNR = 18 dB; (b) filtered constellation diagram; (c) converted binary graph; (d) binary graph after averaging filter.

We have performed numerical simulations for the proposed MFR. 32-Gbaud PM-QPSK, PM-8PSK and PM-16QAM signal were generated and passed through a channel with additive Gaussian white noise. The converted binary image had a size of 100×100 pixels. The threshold for the Voronoi filtering and the size of averaging filter were optimized and kept identical for each modulation format. First, the OSNR value was varied from 10 dB to 30 dB, with a step of 0.2 dB, each having 500 independent implementations. The correct recognition rate was then calculated. Fig. 3(b) and (c) show the correct recognition rate under different OSNR values, and different number of points involved in the MFR. The OSNR, in the latter case, was set to be 15 dB, 22 dB, and 22 dB for QPSK, 8PSK and 16QAM, respectively. It could be noticed that only ~4000 symbols were required to correctly recognize QPSK

and 8PSK, while 16QAM needed ~ 10000 symbols. This might be attributed to the small part of the received symbols on the slicing plane. It was worth noting that the number of symbols required was much fewer than that in the previously reported schemes ($4\text{--}12 \times 10^4$ symbols in [1] and 8×10^4 symbols in [3]).

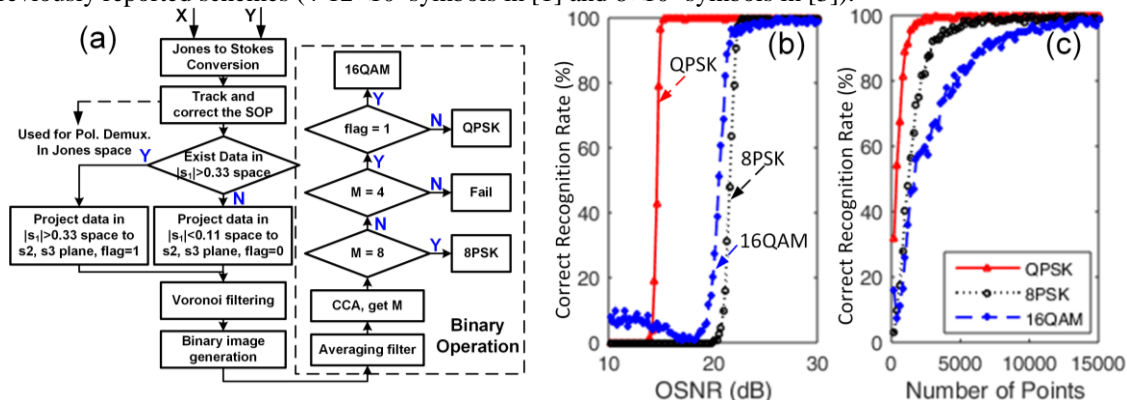


Fig. 3 (a) Flow chart for the CCA based MFR algorithm; (b) & (c) Simulation results of the correct recognition rate under different OSNR values and different number of points.

3. Experiment results

Fig. 4 shows the experimental setup. 32-Gbaud PM QPSK (128 Gbps) and 16QAM (256 Gbps) signal were generated from a programmable pattern generator (PPG) to modulate a 1550-nm continuous-wave from an external cavity laser (ECL), via an in-phase and quadrature modulator. Polarization multiplexing was realized via a polarization multiplexer, which comprised a polarization beam splitter (PBS) to half the signal into two branches, an optical delay line to remove the correlation between x - and y -polarizations and a polarization beam combiner (PBC) to re-combine the signal. The noise was loaded with an 80/20 coupler and a noise source. At the receiver, a tunable optical filter with the 3-dB bandwidth of 0.35 nm was used. Another ECL was used as the local oscillator (LO). A polarization-diversity 90-degree hybrid was used to realize the polarization- and phase-diversity coherent detection of the LO and the received optical signal before balanced detection. The received signal was then sampled at 80 GSamples/s for offline signal processing. 4000 (10000) symbols for QPSK (16QAM) were used for MFR.

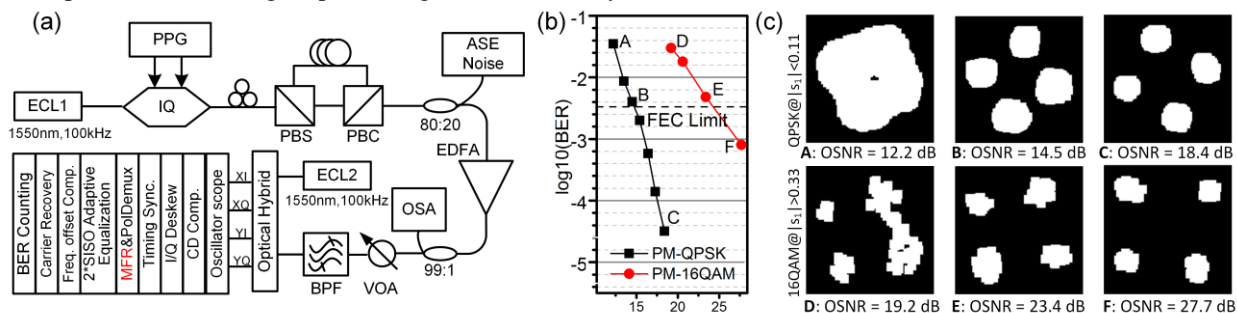


Fig. 4 (a) Experimental setup; (b) bit error rate for PM-QPSK and PM-16QAM signal; (c) the binary images of received data samples A-F in (b) before MFR for PM-QPSK (upper row) and PM-16QAM (lower row).

Fig. 4(b) and (c) shows the experiment results. The bit error rate performances and the final binary images before CCA algorithm were shown. The modulation format of the signal with an OSNR value at around 7% forward error correction limit could be recognized correctly. The experimental results agreed with simulation results very well.

4. Summary

A new low-complexity modulation format recognition method based on connected component analysis technique in computer vision have been proposed and verified, via simulations and experiments, to distinguish between PM-QPSK and PM-16QAM signals.

5. References

- [1] E. J. Adlest, et al, J. Lightwave Technol. vol. 32, no.8, 1501–1509 (2014).
- [2] J. Liu, et al, OFC 2014, paper. Th4D.3
- [3] R. Borkowski, et al, IEEE Photonics Technol. Lett., vol. 25, no. 21, pp. 2129–2132, 2013.
- [4] A. Abubaker, et al, IEEE Signal Processing and Communications, 2007. ICSPC 2007.
- [5] M. Chagnon, et al, Opt. Express 20, 27847–27865 (2012)
- [6] S. Fortune. Algorithmica, 1987, vol. 2, no.1-4, pp. 153–174.